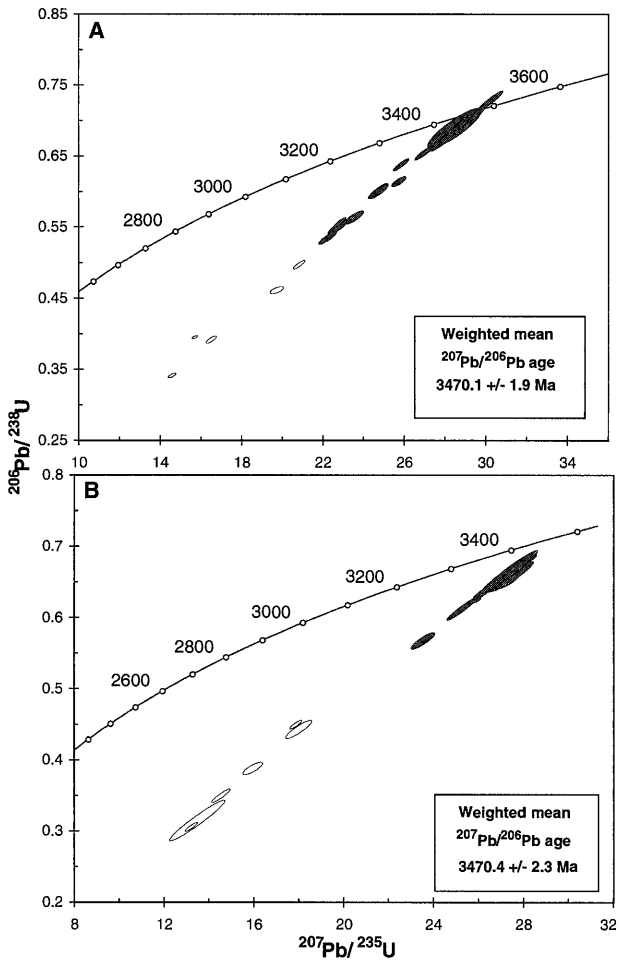

Fig. 2. Concordia diagrams for zircons from the S1 impact layers found in (**A**) the Warrawoona Group of Western Australia and (**B**) the Onverwacht Group of South Africa. Ellipses are 2σ errors, and samples that are greater than 80% concordant (Table 1) are shown shaded. The principal variation in both data sets is the result of modern Pb loss.

References and Notes

1. L. W. Alvarez, W. Alvarez, F. Asaro, H. V. Michel, *Science* **208**, 1095 (1980).
2. N. H. Sleep, K. J. Zahnle, J. F. Kasting, H. J. Morowitz, *Nature* **342**, 139 (1989).
3. A. Y. Glikson, *J. Geodyn.* **32**, 205 (2001).
4. G. Ryder, *Eos* **71**, 313 (1990).
5. T. S. Culler, T. A. Becker, R. A. Muller, P. R. Renne, *Science* **287**, 1785 (2000).
6. D. R. Lowe, G. R. Byerly, *Geology* **14**, 83 (1986).
7. _____, F. Asaro, F. T. Kyte, *Science* **245**, 959 (1989).
8. G. R. Byerly, A. Kroner, D. R. Lowe, W. Todt, M. M. Walsh, *Precambrian Res.* **78**, 125 (1996).
9. J. W. Schopf, *Science* **260**, 640 (1993).
10. D. R. Lowe, *Nature* **284**, 441 (1980).
11. M. M. Walsh, D. R. Lowe, *Nature* **314**, 530 (1985).
12. G. R. Byerly, D. R. Lowe, M. M. Walsh, *Nature* **319**, 489 (1985).
13. D. R. Lowe, G. R. Byerly, *Geology* **15**, 179 (1987).
14. D. R. Lowe *et al.*, *Astrobiology*, in press.
15. A. Shukolyukov *et al.*, in *Impacts and the Early Earth*, I. Gilmour, C. Koeberl, Eds. (Springer-Verlag, Heidelberg, Germany, 2000), pp. 99–116.
16. G. R. Byerly, D. R. Lowe, *Geochim. Cosmochim. Acta* **58**, 3469 (1994).
17. S. W. Hassler, B. M. Simonson, *J. Geol.* **109**, 1 (2001).
18. D. R. Lowe, G. R. Byerly, in *Geologic Evolution of the Barberton Greenstone Belt, South Africa* (Geological Society of America Special Paper 329, Geological Society of America, Boulder, CO, 1999), pp. 1–36.
19. B. F. Bohor, W. J. Betterton, T. E. Krogh, *Earth Planet. Sci. Lett.* **119**, 419 (1993).
20. B. P. Glass, S. B. Liu, *Geology* **29**, 371 (2001).
21. T. E. Krogh, S. L. Kamo, V. L. Sharpton, L. E. Marin, A. R. Hildebrand, *Nature* **366**, 731 (1993).
22. J. C. Dann, *S. Afr. J. Geol.* **103**, 47 (2000).
23. A. Kroner, G. R. Byerly, D. R. Lowe, *Earth Planet. Sci. Lett.* **103**, 41 (1991).
24. M. J. DiMarco, D. R. Lowe, *Precambrian Res.* **44**, 147 (1989).
25. R. I. Thorpe, A. H. Hickman, D. W. Davis, J. K. Mortensen, A. F. Trendall, *Precambrian Res.* **56**, 169 (1992).
26. M. J. Van Kranendonk, P. Morant, *Geol. Surv. West. Aust. Annu. Rep.* **1997**, 55 (1998).
27. R. Buick *et al.*, *Nature* **375**, 574 (1995).
28. S. L. Kamo, D. W. Davis, *Tectonics* **13**, 167 (1994).

29. Supported by grants from the NSF Petrology and Geochemistry Program (G.R.B.) and NASA Astrobiology Program (D.R.L.). We thank Mr. French for access to the Panorama Ranch, Western Australia; Mr. Stamens and Mr. Loock for access to the Songemvelo Park, South Africa; and A. Glikson and M. Walsh for suggestions. This paper is dedicated to the memory of Lunar and Planetary Institute scientist Graham Ryder and his studies of the early solar system's impact history.

Supporting Online Material

www.sciencemag.org/cgi/content/full/297/5585/1325/DC1

Figs. S1 and S2

14 May 2002; accepted 24 June 2002

C–O Bond Formation by Polyketide Synthases

Hyung-Jin Kwon,[1] Wyatt C. Smith,[2] A. Janelle Scharon,[1] Sung Hee Hwang,[2] Mark J. Kurth,[2] Ben Shen[1,2,3]*

Polyketide synthases (PKSs) assemble the polyketide carbon backbone by sequential decarboxylative condensation of acyl coenzyme A (CoA) precursors, and the C–C bond-forming step in this process is catalyzed by the β-ketoacyl synthase (KS) domain or subunit. Genetic and biochemical characterization of the nonactin biosynthesis gene cluster from *Streptomyces griseus* revealed two KSs, NonJ and NonK, that are highly homologous to known KSs but catalyze sequential condensation of the acyl CoA substrates by forming C–O rather than C–C bonds. This chemistry can be used in PKS engineering to increase the scope and diversity of polyketide biosynthesis.

Polyketides are natural products found in bacteria, fungi, and plants that include many clinically important drugs such as erythromycin (antibacterial), daunorubicin and epothilone (anticancer), rapamycin (immunosuppressant), and lovastatin (antihypercholesterolemic). These metabolites are biosynthesized from acyl CoA precursors by PKSs. PKSs have been the focus of intensive research in the past decade for their extraordinary structure, mechanism, and catalytic reactivity and flexibility (*1–4*). Genetic manipulation of PKSs has been increasingly recognized as an alternative strategy for the production of novel compounds that are difficult to access by traditional chemical synthesis (*5–10*). Success of the genetic approach depends on the continuous discovery and characterization of PKSs that catalyze different chemistry (*11–16*).

Three types of PKSs are known. Type I PKSs are multifunctional enzymes that are organized into modules, each of which minimally contains three domains, β-ketoacyl

[1]Division of Pharmaceutical Sciences and [3]Department of Chemistry, University of Wisconsin, Madison, WI 53705, USA. [2]Department of Chemistry, University of California, Davis, CA 95616, USA.

*To whom correspondence should be addressed. E-mail: bshen@pharmacy.wisc.edu

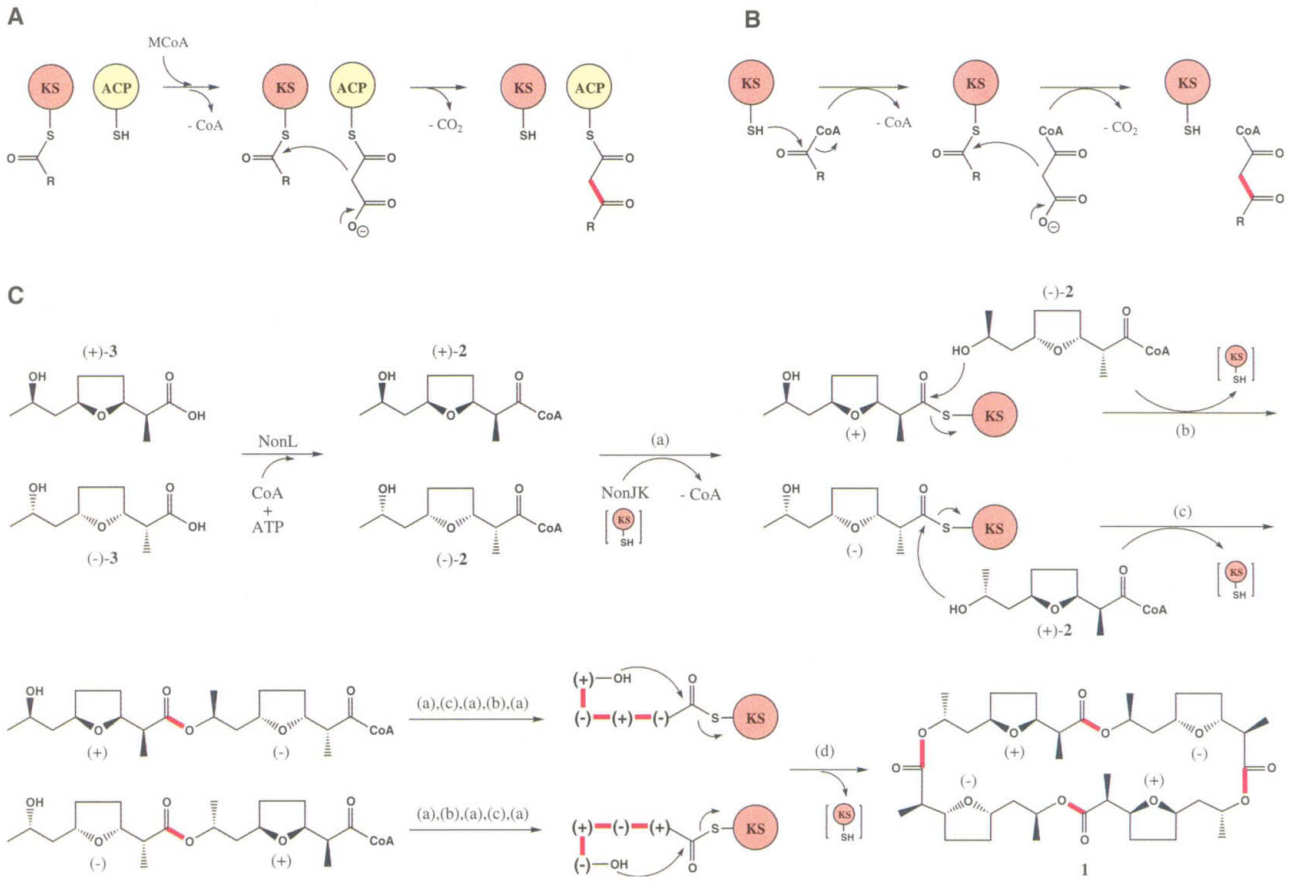

Fig. 1. C–C bond-forming step catalyzed by (**A**) type I and II PKSs and (**B**) type III PKSs and (**C**) C–O bond-forming step catalyzed by the NonJK KSs. The newly formed C–C or C–O bond is shown in red. KS, β-ketoacyl synthase; ACP, acyl carrier protein; CoA, coenzyme A; MCoA, malonyl CoA.

synthase (KS), acyl transferase (AT), and acyl carrier protein (ACP) (*1*, *17*). Type II PKSs are multienzyme complexes minimally consisting of the KSα, KSβ, and ACP subunits (*1*, *18*). [The KSβ unit lacks the conserved Cys residue essential for the KS activity and is also known as chain length factor (*2*) or chain initiation factor (*19*).] Type I and II PKSs share a high degree of amino acid sequence similarity and use ACP to activate the acyl CoA substrates and to channel the growing polyketide intermediates (Fig. 1A). Type III PKSs, also known as chalcone synthase–like PKSs, are essentially KSs (*11*, *13*, *20*). They lack ACP and use acyl CoAs directly as substrates (Fig. 1B). Although type III PKSs have the conserved Cys residue, the amino acid sequences of this Cys motif have no apparent similarity to that of the KSs of the type I and II PKSs. Despite structural and mechanistic differences, all PKSs biosynthesize the polyketide carbon backbone by sequential decarboxylative condensation of acyl CoA precursors, and the KS domain or subunit catalyzes the C–C bond-forming step for polyketide biosynthesis (Fig. 1, A and B).

Here we report two KSs, NonJ and NonK, hereafter referred to as NonJK, that catalyze C–O bond formation in nonactin (Fig. 1C, compound **1**) biosynthesis. The NonJK KSs act on (±)-nonactyl CoA (Fig. 1C, compound **2**), catalyze tetramerization of (+)- and (–)-**2** in a stereospecific (+)(–)(+)(–)-fashion into **1**, and require the Cys residue conserved among all KSs for this reaction (Fig. 1C).

Nonactin belongs to the macrotetrolide family of cyclic polythers that exhibit a broad spectrum of biological activities, including antibacterial, antifungal, antitumor, and immunosuppressive activity. Structurally, **1** is composed of four molecules of (+)- and (–)-nonactic acid (Fig. 1C, compound **3**) in a (+)(–)(+)(–)-macrotetrolide linkage, an intriguing molecular topology not seen in other natural products. The biosynthesis of **1** has been studied by feeding experiments with various isotope-labeled precursors and by cloning and characterizing the biosynthesis gene cluster from *Streptomyces griseus* DSM40695 (*21*–*23*). These studies established that (±)-**3** is synthesized by a PKS that lacks an ACP. The idea that (+)- and (–)-**3** are intermediates in nonactin biosynthesis was supported by their efficient incorporation into **1** and the isolation of both (+)- and (–)-**3**, as well as their dimers, from *S. griseus* fermentation. There are five KS genes within the cluster, *nonJKPQU*, which have deduced products that are highly homologous to KSs of the type II PKS (Fig. 2A) (*22*). Inactivation of any one of them either completely abolishes (*nonJKPQ*) or significantly impairs (*nonU*) **1** production, and expression of any one of them in trans in the corresponding mutants restores **1** production, confirming that all five KS genes are involved in **1** biosynthesis (*24*). Because KSs are only known to catalyze C–C bond-forming steps in polyketide biosynthesis, we reasoned that all KS mutants would retain the enzymatic functions for the C–O bond-forming tetramerization steps involved in (±)-**3** to **1** and, thereby, nonactin production could be restored to all KS mutants by fermenting them in the presence of exogenously added (±)-**3**. That was indeed the case for the *nonPQU* mutants but not for the *nonJK* mutants, suggesting that the NonJK KSs might play a role in the C–O bond-forming steps in nonactin biosynthesis (*24*).

To identify the minimal genes required for the C–O bond-forming tetramerization steps, we combined plasmid-based expression of the *non* genes in *Streptomyces lividans* (fig. S1) with biotransformation of (±)-**3** to **1** in the resultant recombinant strains (*24*). We reasoned that the minimal genes required for the tetramerization step could be identified by successive deletion of genes included in the expression cassettes. Thus, *S. lividans* strains

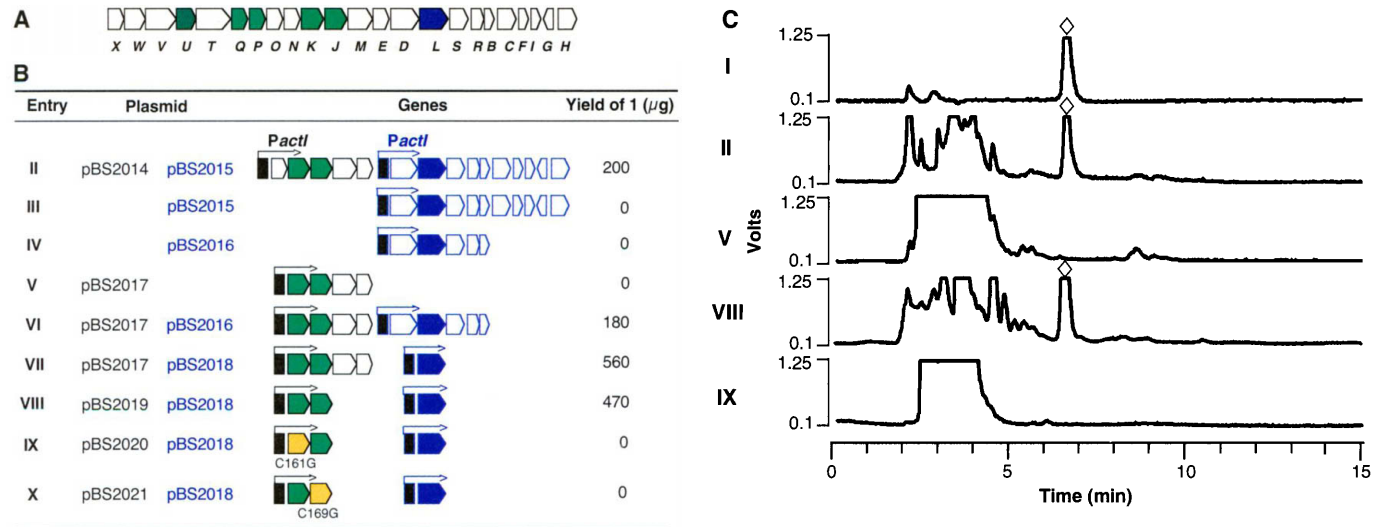

Fig. 2. (**A**) The macrotetrolide biosynthesis gene cluster with the five *nonJKPQU* KS genes shown in green and the *nonL* CoA ligase gene shown in blue. (**B**) Biotransformation of (±)-**3** into **1** by *S. lividans* strains harboring various *non* gene expression cassettes (*24*). Shown in black are gene cassettes constructed in pSET152, and shown in blue are gene cassettes constructed in pWHM3. Black rectangles with arrow indicate orientation of the *actI* promoters. Each entry represents an *S. lividans* strain transformed with either the pSET152- or pWHM3-based cassette or both and its biotransformation yield of **1** from 5 mg of (±)-**3**. The *nonK* C161G and *nonJ* C169G mutants are shown in yellow. (**C**) Examples of HPLC chromatograms of biotransformation of (±)-**3** into **1** by various *S. lividans* recombinant strains: I, authentic **1** standard (white diamond); II, *S. lividans* (pBS2014/pBS2015); V, *S. lividans* (pBS2017); VIII, *S. lividans* (pBS2019/pBS2018); IX, *S. lividans* (pBS2020/pBS2018).

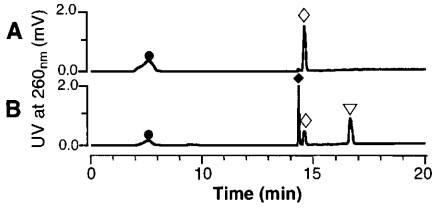

Fig. 3. In vitro synthesis of (±)-**2** from (±)-**3** catalyzed by NonL, requiring ATP and CoA (*24*). (**A**) Negative control in the absence of NonL and (**B**) complete assay with 800 nM NonL. ATP (black dot), AMP (black diamond), CoA (white diamond), (±)-**2** (inverted triangle).

harboring various *non* gene expression cassettes were fermented in the presence of exogenously added (±)-**3** (*21*, *22*, *24*). The production of **1** was monitored by high-performance liquid chromatography (HPLC) and confirmed by electrospray ionization-mass spectrometry (ESI-MS) analysis, yielding a characteristic $(M+Na)^+$ ion at m/z = 759.4, consistent with the molecular formula of $C_{40}H_{64}O_{12}$ for **1** (*21*, *22*). As summarized in Fig. 2, B and C, all recombinant strains expressing *nonJKL* genes are effective in biotransformation of (±)-**3** into **1** (entries II, VI, VII, and VIII), and deletion of *nonJK* or *nonL* from the expression cassettes completely abolishes their biotransformation ability (entries III, IV, and V), suggesting that *nonJKL* genes are essential for this activity. We finally established that *nonJKL* are sufficient for the tetramerization steps by expressing only the *nonJKL* genes; the resultant recombinant strain is as effective in biotransformation of (±)-**3** into **1** (entry VIII) as those strains harboring other *non* genes in addition to *nonJKL*.

On the basis of its high sequence homology to a family of CoA ligases, we reasoned that NonL, rather than directly contributing to the C–O bond-forming steps, instead activates (±)-**3** into CoA esters (±)-**2** that are then tetramerized into **1** by the NonJK KSs. To validate this hypothesis, we expressed *nonL* in *Escherichia coli*, purified NonL as a His_6-tagged fusion protein (fig. S2), and characterized NonL as a CoA ligase (*24*). We monitored the in vitro assay of NonL by HPLC analysis: NonL catalyzes the conversion of (±)-**3** to (±)-**2**, requiring CoA and ATP as co-substrates. Under the condition examined, 80% of (±)-**3** was converted to (±)-**2** in 2 hours, confirming that NonL recognizes both (+)- and (–)-**3** as substrates (Fig. 3). The identity of (±)-**2** was verified by ESI-MS, yielding a characteristic $(M-2H)^{2-}$ ion at m/z = 474.7, consistent with the molecular formula of $C_{31}H_{52}N_7O_{19}P_3S$.

Because NonJKL proteins are sufficient to biotransform (±)-**3** to **1** (Fig. 2, B and C, entry VIII), the characterization of NonL as a CoA ligase, catalyzing the conversion of both (+)- and (–)-**3** into their CoA esters, indicates that NonJK proteins are responsible for the C–O bond-forming tetramerization steps, acting directly on the CoA ester substrates of (+)- and (–)-**2**. KSs known to date catalyze only C–C bond formation, although the CoA substrates can be utilized either directly (by type III PKS) (*11*, *13*, *20*) or indirectly via acyl-ACPs (by both type I and II PKS) (*17*, *18*). Thus, as depicted in Fig. 1C, NonJK, in a mechanistic analogy to type III PKS, could be envisaged to first catalyze the transfer of the nonactyl group from (±)-**2** to the Cys residue of NonJK to form the nonactyl-S-KS species (Fig. 1C, step a). (It remains to be established if NonJ or NonK is enantiospecific for (+)- or (–)-**2**, respectively.) Unlike KSs that catalyze decarboxylative condensation between the carbon anion nucleophile and acyl-S-KS to form the C–C bond (Fig. 1, A and B), the NonJK KSs catalyze the condensation between the oxygen nucleophile of the –OH group of **2** and nonactyl-S-KS to form the C–O bond, yielding the dimers in the form of CoA esters (Fig. 1C, steps b and c). The latter have been isolated as free acids from *S. griseus* fermentation (*25*), supporting the proposed pathway. Iterations of steps a and b or steps a and c eventually lead to the KS-bound linear tetramers that undergo intramolecular condensation between the –OH group of the distal nonactyl unit and the acyl-S-KS carbonyl group to afford **1** (Fig. 1C, step d).

To gain insight into the mechanism of the condensation reaction, we compared the NonJK sequences with those of other KSs of both fatty acid synthases (FASs) and PKSs. All previously characterized KSs contain a Cys-His-His (for type I and II FAS and PKS) (*26*, *27*) or Cys-His-Asn (for type III PKS) (*28*) catalytic triad (Fig. 4). The His-His or His-Asn residues are essential for malonyl-ACP or malonyl CoA decarboxylation to generate the corresponding carbon anion, and the Cys residue catalyzes condensation between the resultant carbon anion and acyl-S-KS to form the C–C bond (Fig. 1, A and B). Strikingly, NonJK are characterized with a

Fig. 4. Alignments of the conserved catalytic residues of NonJK with KSs from FAS, type I and II PKS, and type III PKS. The conserved Cys residue for C–C or C–O bond formation and His-His or His-Asn residues for decarboxylation are highlighted. Protein accession numbers are given after the protein names: FabB, P14926; FabF, P39435; DEBS1, Q03131; PikAIV, AAC69332; Act KSα, CAC44200; Tcm KSα, AAA67515; CHS2, P30074; RppA, BAA33495; NonJ, AAD37451; and NonK, AAD37450.

mutated catalytic triad—Cys-Tyr-His for NonJ or Cys-Gly-His for NonK, suggesting that NonJK lack the decarboxylation activity (Fig. 4). This is consistent with the proposal that NonJK catalyze C–O bond formation by using the –OH as the nucleophile directly. Finally, to confirm that Cys plays a catalytic role in the C–O bond-forming step, we replaced the conserved Cys residue in NonJ or NonK, respectively, with Gly by site-directed mutagenesis (*24*). The resultant mutants completely lose their ability to biotransform (±)-**3** into **1** (Fig. 2, B and C, entries IX and X). Thus, the NonJK KSs catalyze the C–O bond-forming step in nonactin biosynthesis, acting directly on (±)-**2** and using the same active-site residue Cys that is used in KS catalysis of C–C bond formation. Given the high sequence homology and conserved active site between NonJK and other KSs, the structural plasticity and catalytic flexibility of KSs upon protein engineering (*6*, *9*, *10*), and now the C–O bond-forming ability of the NonJK KSs, further mechanistic and structural characterization of the NonJK KSs could allow us to rationally engineer the C–O bond-forming activity into other KSs. This could expand the size and diversity of polyketide library accessible by combinatorial biosynthesis.

References and Notes

1. D. A. Hopwood, *Chem. Rev.* **97**, 2465 (1997).
2. R. McDaniel, S. Ebert-Khosla, D. A. Hopwood, C. Khosla, *Science* **262**, 1546 (1993).
3. B. Shen, C. R. Hutchinson, *Science* **262**, 1535 (1993).
4. A. F. A. Marsden *et al.*, *Science* **263**, 378 (1994).
5. R. Pieper, G. Luo, D. E. Cane, C. Khosla, *Nature* **378**, 263 (1995).
6. R. McDaniel, S. Ebert-Khosla, D. A. Hopwood, C. Khosla, *Nature* **375**, 549 (1995).
7. R. S. Gokhale, S. Y. Tsuji, D. E. Cane, C. Khosla, *Science* **284**, 482 (1999).
8. B. A. Pfeifer, S. J. Admiraal, H. Gramajo, D. E. Cane, C. Khosla, *Science* **291**, 1790 (2001).
9. D. E. Cane, C. T. Walsh, C. Khosla, *Science* **282**, 63 (1998).
10. J. M. Jez *et al.*, *Chem. Biol.* **7**, 919 (2000).
11. S. Eckermann *et al.*, *Nature* **396**, 387 (1998).
12. J. Kennedy *et al.*, *Science* **284**, 1368 (1999).
13. N. Funa *et al.*, *Nature* **400**, 897 (1999).
14. J. G. Metz *et al.*, *Science* **293**, 290 (2001).
15. W. Liu, S. D. Christenson, S. Standage, B. Shen, *Science* **297**, 1170 (2002).
16. J. Ahlert *et al.*, *Science* **297**, 1173 (2002).
17. J. Staunton, K. J. Weissman, *Nat. Prod. Rep.* **18**, 380 (2001).
18. B. Shen, *Top. Curr. Chem.* **209**, 1 (2000).
19. C. Bisang *et al.*, *Nature* **401**, 502 (1999).
20. J. Schröder, in *Comprehensive Natural Products Chemistry*, D. Barton, K. Nakanish, O. Meth-Cohn, Eds. (Elsevier, New York, 1999), vol. 1, pp. 749–771.
21. W. C. Smith, L. Xiang, B. Shen, *Antimicrob. Agents Chemother.* **44**, 1809 (2000).
22. H.-J. Kwon, W. C. Smith, L. Xiang, B. Shen, *J. Am. Chem. Soc.* **123**, 3385 (2001).
23. M. E. Nelson, N. D. Priestley, *J. Am. Chem. Soc.* **124**, 2894 (2002).
24. Supplementary figures and additional information about materials and methods are available on *Science* Online.
25. W. F. Fleck, M. Ritzau, S. Heinze, U. Gräfe, *J. Basic Microbiol.* **36**, 235 (1996).
26. M. He, M. Varoglu, D. H. Sherman, *J. Bacteriol.* **182**, 2619 (2000).
27. J. G. Olsen *et al.*, *FEBS Lett.* **460**, 46 (1999).
28. J. M. Jez, J.-L. Ferrer, M. E. Bowman, R. A. Dixon, J. P. Noel, *Biochemistry* **39**, 890 (2000).

29. Supported in part by a CAREER award (MCB9733938) from NSF to B.S. B.S. is a recipient of an Independent Scientist Award (AI51689) from NIH. A.J.S. was supported in part by NIH grant T32 GM08505.

Supporting Online Material
www.sciencemag.org/cgi/content/full/297/5585/1327/DC1
Materials and Methods
Figs. S1 and S2

23 April 2002; accepted 12 July 2002

Structure of the Extracellular Region of HER3 Reveals an Interdomain Tether

Hyun-Soo Cho and Daniel J. Leahy*

We have determined the 2.6 angstrom crystal structure of the entire extracellular region of human HER3 (ErbB3), a member of the epidermal growth factor receptor (EGFR) family. The structure consists of four domains with structural homology to domains found in the type I insulin-like growth factor receptor. The HER3 structure reveals a contact between domains II and IV that constrains the relative orientations of ligand-binding domains and provides a structural basis for understanding both multiple-affinity forms of EGFRs and conformational changes induced in the receptor by ligand binding during signaling. These results also suggest new therapeutic approaches to modulating the behavior of members of the EGFR family.

The epidermal growth factor receptor (EGFR) is the founding member of the ErbB family of receptor tyrosine kinases that in humans includes HER1 (EGFR, ErbB1), HER2 (Neu, ErbB2), HER3 (ErbB3), and HER4 (ErbB4) (*1*–*4*). These receptors respond to EGF and related ligands to mediate cellular growth and differentiation in multiple tissues in both the developing embryo and adult (*5*–*8*). Loss of any of the ErbB family members results in embryonic lethality in mice with defects observed in organs including the brain, heart, skin, lung, and gastrointestinal tract, depending on the receptor affected (*7*). Overexpression and activation of ErbB receptors, most notably HER1 and HER2, are found in many human cancers and are critical factors in the development and malignancy of these tumors (*9*). Therapies that target these receptors have shown promise, and a monoclonal antibody against HER2, with the trade name Herceptin, is currently being used to treat breast cancer (*10*).

ErbB receptors consist of an ~620–amino acid extracellular region followed by a single transmembrane-spanning region and a cytoplasmic kinase domain. The extracellular regions of ErbB receptors are made up of four domains arranged as a tandem repeat of a two-domain unit consisting of an ~190–amino acid L domain followed by an ~120–amino acid cysteine-rich domain. The first three of these domains share 15 to 20% sequence identity with the first three domains of the type I insulin-like growth factor receptor (IGFR), for which a structure is known (*11*). Unlike the homologous region of HER1, an NH_2-terminal three-domain frag-

Department of Biophysics and Biophysical Chemistry, Howard Hughes Medical Institute, Johns Hopkins University School of Medicine, 725 North Wolfe Street, Baltimore, MD 21205, USA.

*To whom correspondence should be addressed. E-mail: leahy@groucho.med.jhmi.edu